Simulation of vortex sheet roll-up: chaos, azimuthal waves, ring merger

Robert KRASNY[1], Keith LINDSAY[2] & Monika NITSCHE[3]

[1]*University of Michigan, Department of Mathematics, Ann Arbor, Michigan 48109-1109 USA*
krasny@umich.edu

[2]*National Center for Atmospheric Research, Climate and Global Dynamics Boulder, Colorado 80307-3000 USA*

[3]*University of New Mexico, Department of Mathematics and Statistics Albuquerque, New Mexico 87131-1141 USA*

Abstract This article reviews some recent simulations of vortex sheet roll-up using the vortex blob method. In planar and axisymmetric flow, the roll-up is initially smooth but irregular small-scale features develop later in time due to the onset of chaos. A numerically generated Poincaré section shows that the vortex sheet flow resembles a chaotic Hamiltonian system with resonance bands and a heteroclinic tangle. The chaos is induced by a self-sustained oscillation in the vortex core rather than external forcing. In three-dimensional flow, an adaptive treecode algorithm is applied to reduce the CPU time from $O(N^2)$ to $O(N \log N)$, where N is the number of particles representing the sheet. Results are presented showing the growth of azimuthal waves on a vortex ring and the merger of two vortex rings.

Vortex blob methods discrete,
Applied to roll-up of a sheet,
Will persuade any cynic
That heteroclinic
Tangles give insights quite neat.

1. Introduction

Vortex sheets are commonly used in fluid dynamics to model thin shear layers in slightly viscous flow. This article reviews some recent simulations of vortex sheet roll-up in planar, axisymmetric, and three-dimensional flow Krasny & Nitsche 2001; Lindsay & Krasny 2001. Vortex sheet simulations encounter difficulties due to Kelvin-Helmholtz instability and singularity formation Moore 1979 and the present work deals with these issues by applying the vortex blob method Chorin & Bernard 1973; Anderson 1985; Krasny 1987. This approach regularises

K. Bajer and H.K. Moffatt (eds.), Tubes, Sheets and Singularities in Fluid Dynamics, 3–12.

the singular Biot-Savart kernel in the integral defining the sheet velocity. As a result, the instability is diminished and the computations can proceed past the singularity formation time into the roll–up regime. A comprehensive review of vortex blob methods is given by Cottet & Koumoutsakos (2000).

The article is organised as follows. The onset of chaos in planar and axisymmetric flow is discussed in §2. A treecode algorithm for vortex sheet motion in three-dimensional flow is described in §3 and results are presented showing the growth of azimuthal waves on a vortex ring and the merger of two vortex rings. A summary is given in §4.

2. The onset of chaos in vortex sheet flow

In planar flow, a vortex sheet is a material curve and it is represented on the discrete level by a set of particles $\mathbf{x}_i(t)$ with scalar weights α_i, for $i = 1, \ldots, N$. The particles are advected by the equations

$$\frac{d\mathbf{x}_i}{dt} = \sum_{j=1}^{N} \alpha_j \mathbf{K}_\delta(\mathbf{x}_i, \mathbf{x}_j) \ . \tag{1}$$

where

$$\mathbf{K}_\delta(\mathbf{x}, \mathbf{y}) = -\frac{1}{2\pi} \frac{(\mathbf{x} - \mathbf{y})^\perp}{\left(|\mathbf{x} - \mathbf{y}|^2 + \delta^2\right)} \tag{2}$$

is a regularised form of the 2-D Biot-Savart kernel. A similar approach is used for axisymmetric flow Nitsche & Krasny 1994.

Figure 1 displays the roll-up of an initially flat vortex sheet in planar and axisymmetric flow, yielding respectively a vortex pair and a vortex ring Krasny & Nitsche 2001. At early times the roll–up is smooth, but at late times the sheet develops irregular small-scale features; a wake is shed behind the vortex ring arid gaps form between the spiral turns in the spiral core in both cases. Figure 2 shows a close-up at the final time. In the planar case, the irregular features are confined to a thin annular band around the core. In the axisymmetric case, the irregular features in the core are more dispersed and the sheet folds and stretches near the rear. It should be noted that the computations are well-resolved. As explained below, the irregular features are due to the onset of chaos.

It is well-known that the motion of material points in planar incompressible flow is governed by a Hamiltonian system,

$$\frac{\mathrm{d}x}{\mathrm{d}t} = \frac{\partial \psi}{\partial y}, \qquad \frac{\mathrm{d}y}{\mathrm{d}t} = -\frac{\partial \psi}{\partial x}, \tag{3}$$

where the stream function $\psi(x, y, t)$ plays the role of the Hamiltonian. A similar result holds for axisymmetric flow. Insights from dynamical

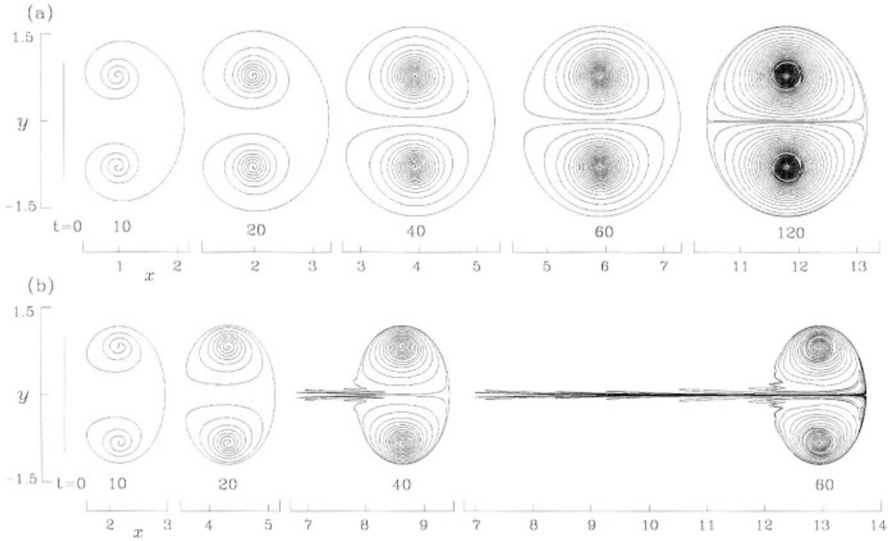

Figure 1. Computed vortex sheet roll-up ($\delta = 0.2$). (a) planar vortex pair; (b) axisymmetric vortex ring.

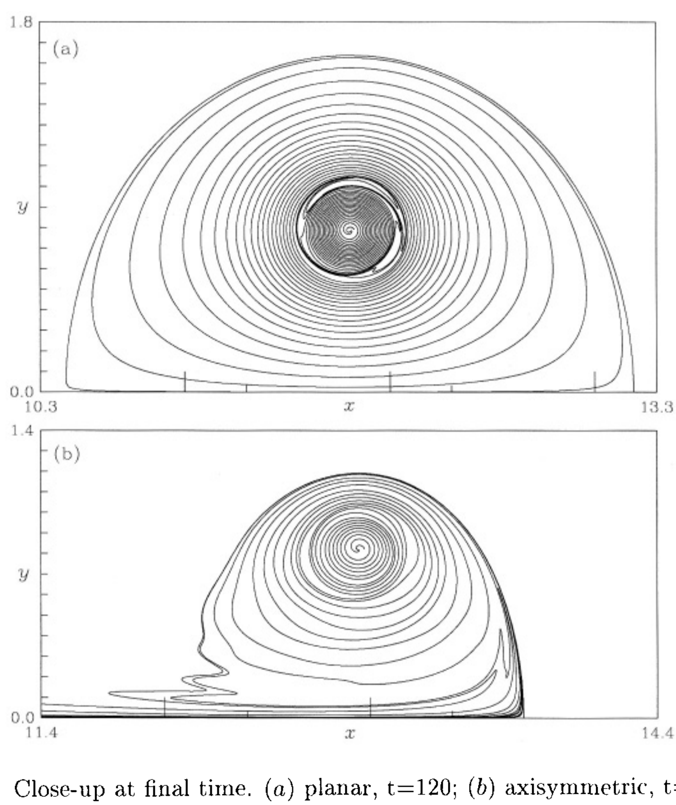

Figure 2. Close-up at final time. (a) planar, t=120; (b) axisymmetric, t=60.

systems theory can then be used to shed light on the fluid dynamics Aref 1984; Ottino 1989.

One example especially relevant for the present work is the oscillating vortex pair Rom-Kedar, Leonard & Wiggins 1990. The stream function in this model has the form

$$\psi(x,y,t) = \psi_0(x,y) + \epsilon\,\psi_1(x,y,t), \tag{4}$$

where $\psi_0(x,y)$ is the steady flow defined by a pair of counter-rotating point-vortices, $\psi_1(x,y,t)$ is a time-periodic perturbation strain field, and ϵ is the perturbation amplitude. The system is integrable for $\epsilon = 0$ and chaotic for $\epsilon > 0$. Figure 3 describes the dynamics of the model. In particular, the perturbed system has chaotic orbits associated with heteroclinic tangles and resonance bands Guckenheimer & Holmes 1983; Wiggins 1992.

Returning to the vortex sheet flow, the first observation is that past the initial transient the flow enters a quasisteady state. In this regime it was found that the vortex core undergoes a small-amplitude oscillation which is close to time-periodic. In other words, the stream function of the vortex sheet flow is close to the form given in (4). Using the oscillation frequency, a Poincaré section of the vortex sheet flow was constructed and the result, shown in figure 4, has the generic features of a chaotic Hamiltonian system. The resonance bands and heteroclinic tangle in the Poincaré section are well–correlated with the irregular features in the shape of the vortex sheet (compare figures 2 and 4). Hence the vortex sheet flow resembles a chaotic Hamiltonian system, although the chaos is induced here by a self-sustained oscillation in the vortex core rather than external forcing. The oscillation resembles the periodic motion of a strained elliptic vortex Kida 1981.

3. Azimuthal waves, vortex ring merger

In three-dimensional flow, a vortex sheet is a material surface and it is represented on the discrete level by a set of particles $\mathbf{x}_i(t)$ with vector-valued weights $\mathbf{w}_i$, for $i = 1, \ldots, N$. The particles are advected by the equations

$$\frac{d\mathbf{x}_i}{dt} = \sum_{j=1}^{N} \mathbf{K}_\delta(\mathbf{x}_i, \mathbf{x}_j) \times \mathbf{w}_j \;, \tag{5}$$

where

$$\mathbf{K}_\delta(\mathbf{x},\mathbf{y}) = -\frac{1}{4\pi}\frac{\mathbf{x}-\mathbf{y}}{(|\mathbf{x}-\mathbf{y}|^2 + \delta^2)^{3/2}} \tag{6}$$

is a regularized form of the 3-D Biot-Savart kernel Rosenhead 1930; Moore 1972. Evaluating the sum (5) for $i = 1, \ldots, N$ is an example of

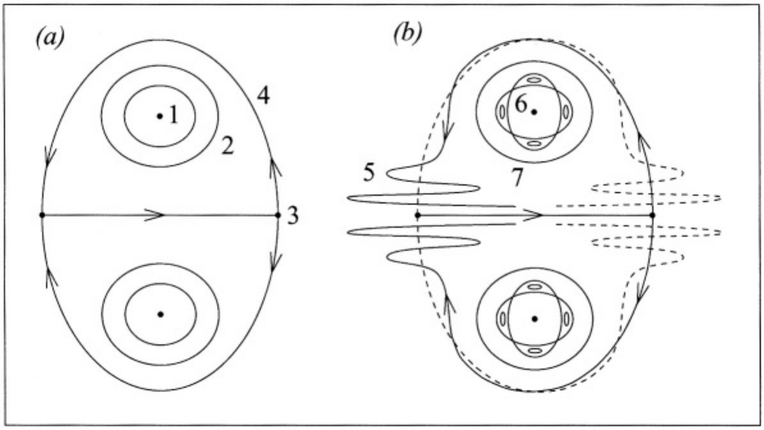

Figure 3. Dynamics of an oscillating vortex pair Rom-Kedar, Leonard & Wiggins 1990. A Poincaré section is plotted schematically. (a) $\epsilon = 0$; (b) $\epsilon > 0$. 1: elliptic point, 2: periodic orbit, 3: hyperbolic point, 4: homoclinic orbit, 5: heteroclinic tangle, 6: resonance band, 7: KAM curve.

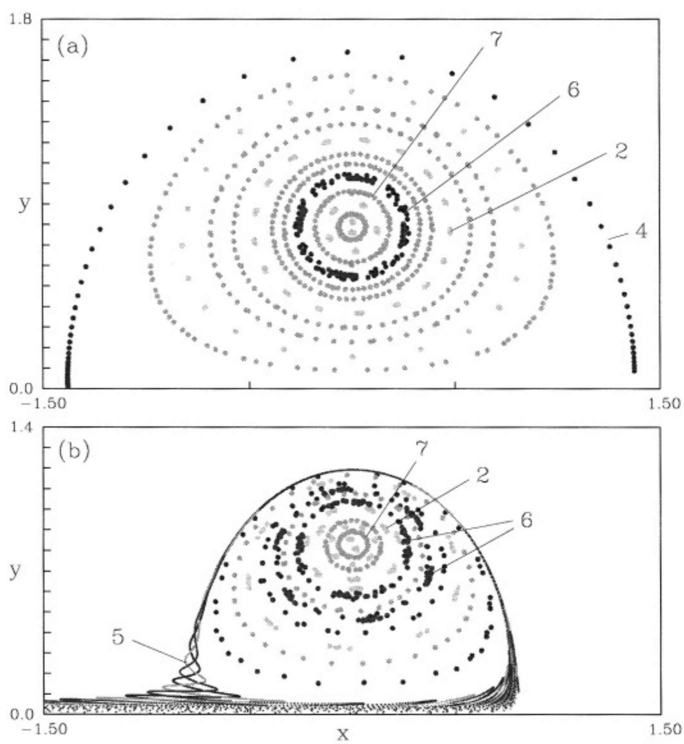

Figure 4. Poincaré section of the vortex sheet flow. (a) planar; (b) axisymmetric. The labels are the same as in figure 3. The vortex sheet flow has the generic features of a chaotic Hamiltonian system (resonance bands, heteroclinic tangle, KAM curves).

an N-body problem. The simplest evaluation procedure is direct summation which computes $O(N^2)$ particle-particle interactions per timestep. Since new particles are inserted to maintain resolution as the sheet rolls up, the CPU time quickly becomes prohibitive.

The present simulations used a treecode algorithm to reduce the cost of evaluating the particle velocities Lindsay & Krasny 2001. The particles are divided into a nested set of clusters and the $O(N^2)$ particle-particle interactions are replaced by a smaller number of particle-cluster interactions which can be efficiently computed using a multipole approximation. Treecode algorithms reduce the cost to $O(N \log N)$ Barnes & Hut 1986 or $O(N)$ Greengard &; Rokhlin 1987. The algorithm used here follows an approach developed for two-dimensional vortex sheet motion and applies Taylor series in Cartesian coordinates to approximate the regularized Biot-Savart kernel Draghicescu & Draghicescu 1995. The algorithm implements several adaptive techniques including variable order approximation, nonuniform rectangular clusters, and a run-time choice between Taylor approximation and direct summation. The results presented below used up to $N \approx 3.5 \cdot 10^5$ particles.

Figure 5 shows the growth of azimuthal waves on a vortex ring. The initial condition is a circular-disk vortex sheet with a transverse azimuthal perturbation of wavenumber $k = 9$. Such waves have been observed in experiments Lim & Nickels 1995; Shariff & Leonard 1992.

Figure 6 presents a simulation of vortex ring merger. Experiments show that two vortex rings moving side by side in the same direction draw close to each other and merge into a single ring Schatzle 1987. This is a popular test case for numerical methods Cottet & Koumoutsakos 2000 and there is much interest in this flow as an example of vortex reconnection Kida & Takaoka 1994. In the present simulation, the rings are formed by the roll-up of two initially flat circular-disk vortex sheets. In figure 6, the material sheet surfaces are plotted in column (a) and the associated vorticity isosurfaces are plotted in columns (b, c). The vorticity was computed by differentiating the regularized Biot-Savart velocity integral. Two isosurfaces are plotted, $\frac{1}{3}$ (light gray) and $\frac{2}{3}$ (dark gray) of the initial maximum vorticity amplitude. The material surfaces representing the sheets approach closely but they do not actually touch. On the other hand, the vorticity isosurfaces apparently cancel and reconnect as the rings approach each other.

Figure 7 shows a closeup of the material surfaces in the ring merger simulation at the final time. In the region where the two rings approach closely the core radius is small. The irregular small-scale features appearing in this region are artifacts of the graphics software; the simulation is well-resolved. The core radius becomes larger away from this region.

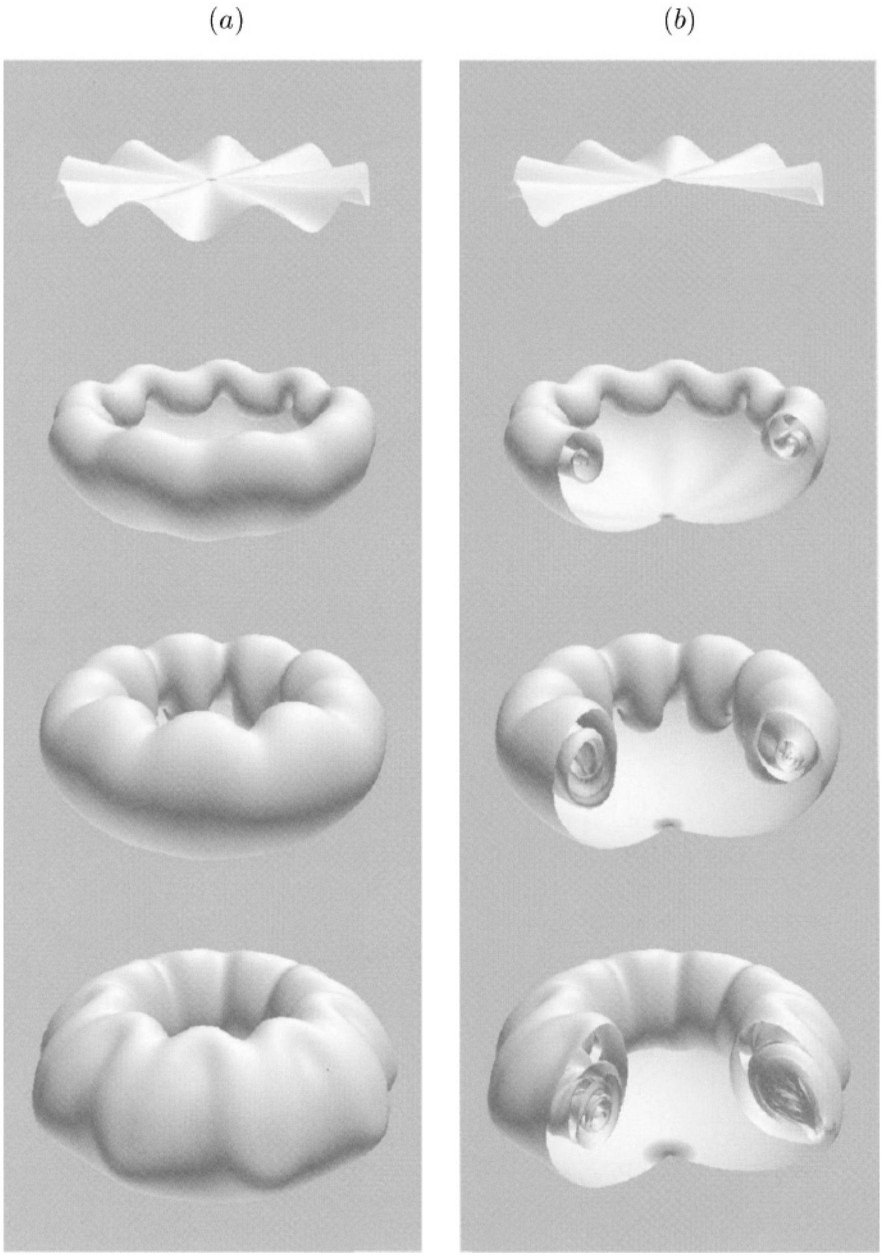

Figure 5. The growth of azimuthal waves on a vortex ring. The initial condition is a circular-disk vortex sheet with a transverse azimuthal perturbation of wavenumber $k = 9$ ($\delta = 0.1$). (*a*) complete sheet; (*b*) section. Time increases going down the page, $t = 0, 2, 4, 6$.

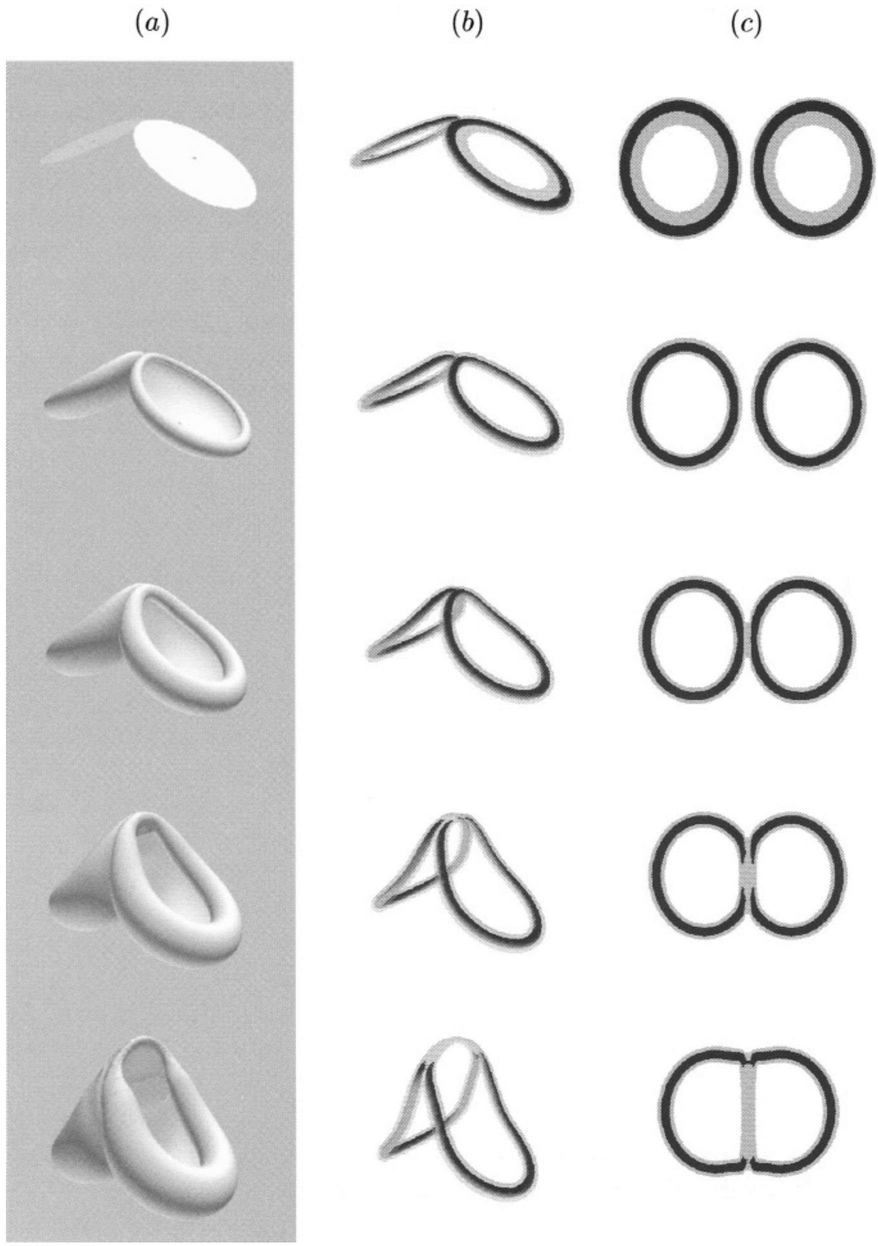

Figure 6. Simulation of vortex ring merger. Two rings are formed by the roll-up of initially flat circular-disk vortex sheets. (a) material surfaces; (b, c) vorticity isosurfaces (perspective, top view). Time increases going down the page, $t = 0, 1, 2, 3, 4$.

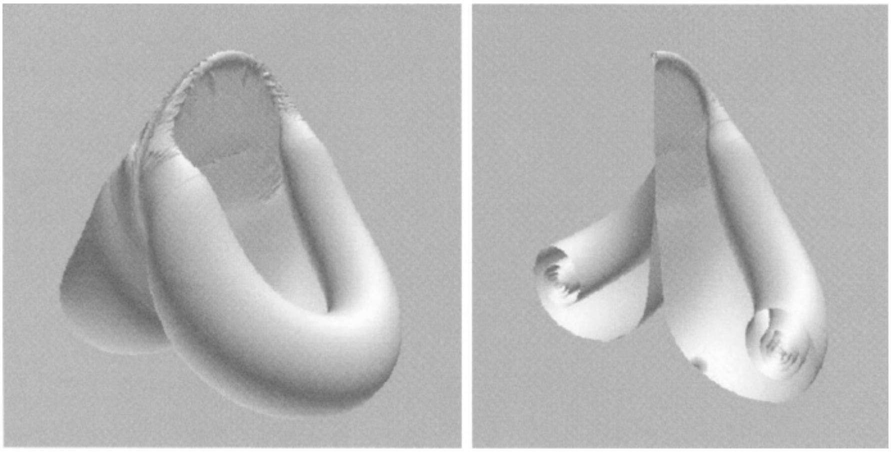

Figure 7. Closeup of material sheet surfaces in the ring merger simulation; $t = 4.5$. (a) complete surface; (b) section.

4. Summary

Simulations of vortex sheet roll-up using the vortex blob method were presented. In planar and axisymmetric flow, the sheet develops irregular small-scale features due to the onset of chaos. A Poincaré section of the vortex sheet flow displays resonance bands and a heteroclinic tangle, the generic features of a chaotic Hamiltonian system. The chaos is induced by a self-sustained oscillation in the vortex core rather than external forcing. In three-dimensional flow, a treecode algorithm is applied to simulate the growth of azimuthal waves on a vortex ring and the merger of two vortex rings. In the latter case, the vorticity isosurfaces cancel and reconnect even though the material sheet surfaces do not touch. The simulation is nominally inviscid and apparently it is the regularized Biot-Savart integration that allows the vorticity to cancel. There is evidence that vortex blob simulations provide a good approximation for true viscous flow in certain cases Nitsche &; Krasny 1994; Tryggvason, Dahm & Sbeih 1991, but it will be necessary to perform comparisons with experiments and Navier-Stokes simulations to determine the physical validity of the present findings.

Acknowledgments

This work was supported by the U. S. National Science Foundation through grants DMS-9506452, DMS-9996254, and DMS-0107187.

References

ANDERSON, C. R. 1985 A vortex method for flows with slight density variations. *Comput. Phys.* **61**, 417–444.

AREF, H. 1984 Stirring by chaotic advection. *J. Fluid Mech.* **143**, 1–21.

BARNES, J. & HUT, P. 1986 A hierarchical *O*(*N* log *N*) force-calculation algorithm. *Nature* **324**, 446–449.

CHORIN, A. J. & BERNARD, P. S. 1973 Discretization of a vortex sheet, with an example of roll-up, *J. Comput. Phys.* **13**, 423–429.

COTTET, G.-H. & KOUMOUTSAKOS, P. D. 2000 *Vortex Methods: Theory and Practice.* Cambridge University Press.

DRAGHICESCU, C. & DRAGHICESCU, M. 1995 A fast algorithm for vortex blob interactions, *J. Comput. Phys.* **116**, 69–78.

GREENGARD, L. & ROKHLIN, V. 1987 A fast algorithm for particle simulations, *J. Comput. Phys.* **73**, 325–348.

GUCKENHEIMER, J. & HOLMES, P. 1983 *Nonlinear Oscillations, Dynamical Systems, and Bifurcations of Vector Fields.* Springer-Verlag.

KIDA, S. 1981 Motion of an elliptic vortex in a uniform shear flow. *J. Phys. Soc. Jpn.* **50**, 3517–3520.

KIDA, S. & TAKAOKA, M. 1994 Vortex reconnection, *Annu. Rev. Fluid Mech.* **26**, 169–189.

KRASNY, R. 1987 Computation of vortex sheet roll-up in the Trefftz plane. *J. Fluid Mech.* **184**, 123–155.

KRASNY, R. & NITSCHE, M. 2001 The onset of chaos in vortex sheet flow. *J. Fluid Mech.* **454**, 47–69.

LIM, T. T. & NICKELS, T. B. 1995 Vortex rings. In *Fluid Vortices* (ed. S. I. Green), pp. 95–153. Kluwer.

LINDSAY, K. & KRASNY, R. 2001 A particle method and adaptive treecode for vortex sheet motion in three-dimensional flow. *J. Comput. Phys.* **172**, 879–907.

MOORE, D. W. 1972 Finite amplitude waves on aircraft trailing vortices, *Aero. Quart.* **23**, 307–314.

MOORE, D. W. 1979 The spontaneous appearance of a singularity in the shape of an evolving vortex sheet. *Proc. Roy. Soc. Land.* A **365**, 105–119.

NITSCHE, M. & KRASNY, R. 1994 A numerical study of vortex ring formation at the edge of a circular tube, *J. Fluid Mech.* **276**, 139–161.

OTTINO, J. M. 1989 *The Kinematics of Mixing: Stretching, Chaos, and Transport.* Cambridge University Press.

ROM-KEDAR, V., LEONARD, A. & WIGGINS, S. 1990 An analytical study of transport, mixing and chaos in an unsteady vortical flow. *J. Fluid Mech.* **314**, 347–394.

ROSENHEAD, L. 1930 The spread of vorticity in the wake behind a cylinder, *Proc. Roy. Soc. Land.* A**127**, 590–612.

SCHATZLE, P. R. 1987 An experimental study of fusion of vortex rings, *Ph.D. Thesis,* California Institute of Technology.

SHARIFF, K. & LEONARD, A. 1992 Vortex rings. *Ann. Rev. Fluid Mech.* **24**, 235–297.

TRYGGVASON, G., DAHM, W. J. A. & SBEIH, K. 1991 Fine structure of vortex sheet rollup by viscous and inviscid simulations, *ASME J. Fluid Engin.* **113**, 31–36.

WIGGINS, S. 1992 *Chaotic Transport in Dynamical Systems.* Springer-Verlag.